Design of Liquid-Liquid Phase Transfer Catalytic Processes

Ketan D. Samant, Divya J. Singh, and Ka M. Ng
Dept. of Chemical Engineering, University of Massachusetts, Amherst, MA 01003

Issues related to the conceptual design of liquid-liquid phase transfer catalytic (LLPTC) processes are discussed. Based on a generic mathematical model, effects of reaction kinetics and mass transfer on the performance of LLPTC processes are captured in terms of Damköhler numbers. The effects of thermodynamic parameters on the process performance are also discussed. Elucidation of the basic mechanisms leads to the synthesis of two classes of flowsheets for LLPTC processes with recovery and recycle of the phase transfer catalyst. Salient features of operation are identified for both classes. The use of the model in making judicious choices of the reactor phase attributes, the catalyst recovery scheme, the catalyst, and the organic solvent is demonstrated.

Introduction

Phase-transfer catalysis (PTC) uses catalytic amounts of phase-transfer agents to facilitate reactions between reagents in two immiscible phases. The foundations of phase-transfer catalysis were laid by the studies of Starks (1971), Makosza (1975), and Brändström (1977). Since then, PTC has provided an economically profitable and environmentally benign route for synthesizing a wide variety of organic chemicals, particularly in the fine chemicals industry (Reuben and Sjöberg, 1981; Freedman, 1986; Starks et al., 1994; Naik and Doraiswamy, 1998).

Despite its advantages, there are barriers to the commercialization of PTC processes. Experimental studies have been the chief driving force behind most of the industrial applications in this area. Although extremely important, these studies by themselves are not adequate for efficient and optimal development of PTC technology. Yet, as pointed out by Naik and Doraiswamy (1998), the engineering analysis needed to complement an experimental program has been limited to a handful of articles on kinetic modeling of batch PTC reactions.

The objective of this article is to provide a foundation that can be used in conjunction with the insights obtained from experimental studies and the existing empirical knowledge for the design of PTC processes. As the first building block, we will use the stirred cell model (Samant and Ng, 1998b) for liquid-liquid PTC (LLPTC) processes. With the help of this model, we will try to understand the interplay of reactions, mass transfer, and thermodynamics, and their effects on the reactor performance. We will show how these effects are governed by the dimensionless Damköhler numbers for reaction and mass transfer, and by the thermodynamic parameters. On the basis of the results, we will also develop feasible flowsheets for recovery and recycle of phase transfer (PT) catalysts. As the next building block, we will provide guidelines for choosing phase attributes such as the choice of dispersed and continuous phases, the average drop size, the phase holdups, and the residence times; and process attributes such as catalyst and solvent type.

Mathematical Model

Consider a liquid-liquid phase transfer catalytic system as shown in Figure 1a. We have an organic phase reaction

$$RY + QX \Leftrightarrow RX + QY, \tag{1}$$

where RY is the reactant that is to be converted into product RX. The reaction occurs in the presence of an organic solvent I. The aqueous phase contains salts MX, MY, QX, and QY dissolved in water W. QX and QY represent the phase transfer catalyst. The phase transfer catalytic mechanism helps in bringing the cation X^- over to the organic phase in

Correspondence concerning this article should be addressed to K. M. Ng at Dept. of Chemical Engineering, Hong Kong University of Science and Technology, Clear Water Bay, Hong Kong.
Current address for K. D. Samant: Aspen Technology, Inc., Ten Canal Park, Cambridge, MA 02141-2201.

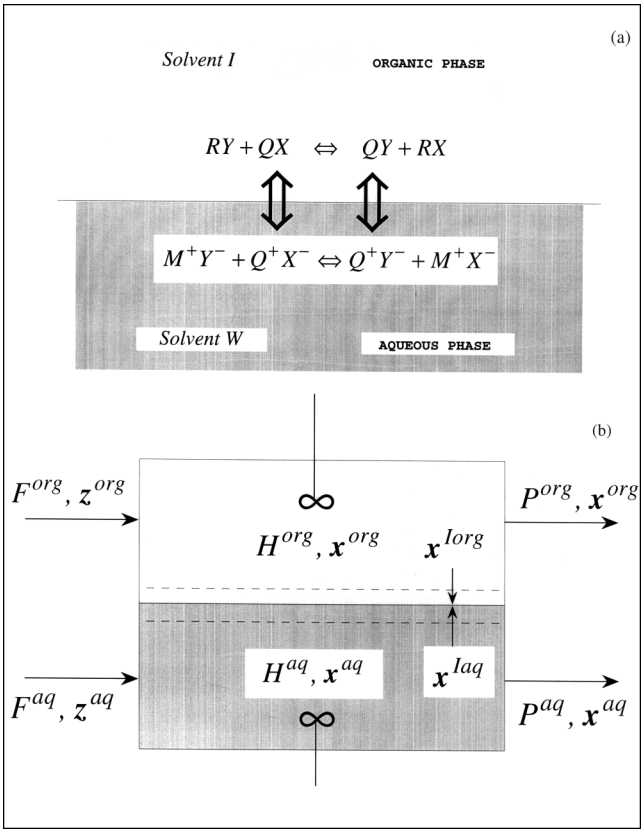

Figure 1. Liquid-liquid phase transfer catalytic (LLPTC) processes.

(a) Mechanism; (b) stirred cell model.

form of the salt QX. This system represents very well most of the industrial LLPTC processes carried out under neutral conditions. Although we consider only one stoichiometrically balanced organic phase reaction here, as is the case with the majority of LLPTC processes, multiple reactions and reactions with different stoichiometries can be easily considered.

Real and apparent mole fractions

Typically, the salts are completely dissociated in the aqueous phase, but do not dissociate (exist as ion pairs) in the organic phase (Dehmlow and Dehmlow, 1993). In addition, we assume that the organic-phase components RY, RX, and I do not go into the aqueous phase and the aqueous-phase components, W, and the hydrophilic cation M^+ do not go into the organic phase. Therefore, the aqueous phase contains components Q^+, M^+, X^-, Y^-, and water W and the organic phase has components RX, RY, solvent I, and ion pairs QX and QY. For a consistent mathematical representation, it is convenient to have the same components in both phases. What this implies is that, although QX and QY exist as ion-pairs in the organic phase, we must consider them not as QX and QY, but as Q^+, X^-, and Y^-. RX, RY, QX, QY, and I are the *real* components in the organic phase and we will refer to their mole fraction as *real* mole fractions. RX, RY, Q^+, X^-, Y^-, and I are the *apparent* components and their mole fractions are called *apparent* mole fractions.

To relate the real mole fractions to the apparent mole fractions, let us denote the number of moles of real components in the organic phase by $\hat{n}_i^{\text{org}}$, $i = RX$, RY, QX, QY, I and the number of moles of apparent components in the organic phase by n_i^{org}, $i = RX$, RY, Q^+, X^-, Y^-, I. By observation, we can write

$$
\begin{aligned}
n_{RX}^{\text{org}} &= \hat{n}_{RX}^{org} \\
n_{RY}^{\text{org}} &= \hat{n}_{RY}^{\text{org}} \\
n_{I}^{\text{org}} &= \hat{n}_{I}^{\text{org}} \\
n_{Q^+}^{\text{org}} &= \hat{n}_{QX}^{\text{org}} + \hat{n}_{QY}^{\text{org}} \\
n_{X^-}^{\text{org}} &= \hat{n}_{QX}^{\text{org}} \\
n_{Y^-}^{\text{org}} &= \hat{n}_{QY}^{\text{org}}.
\end{aligned} \tag{2}
$$

Therefore, we have

$$
\begin{aligned}
& \hat{n}_{TOT}^{\text{org}} = \hat{n}_{RX}^{\text{org}} + \hat{n}_{RY}^{\text{org}} + \hat{n}_{I}^{\text{org}} + \hat{n}_{QX}^{\text{org}} + \hat{n}_{QY}^{\text{org}} \\
\Rightarrow \quad & \hat{n}_{TOT}^{\text{org}} = n_{RX}^{\text{org}} + n_{RY}^{\text{org}} + n_{I}^{\text{org}} + n_{X^-}^{\text{org}} + n_{Y^-}^{\text{org}} \\
\Rightarrow \quad & \hat{n}_{TOT}^{\text{org}} = n_{TOT}^{\text{org}} - n_{Q^+}^{\text{org}}.
\end{aligned} \tag{3}
$$

Using these equations the real mole fractions $\hat{x}_i^{\text{org}}$ can be written in terms of the apparent mole fractions x_i^{org} as

$$
\begin{aligned}
\hat{x}_{QX}^{\text{org}} &= \frac{\hat{n}_{QX}^{\text{org}}}{\hat{n}_{TOT}^{\text{org}}} = \frac{n_{X^-}^{\text{org}}}{n_{TOT}^{\text{org}}} \frac{n_{TOT}^{\text{org}}}{\hat{n}_{TOT}^{\text{org}}} = \frac{x_{X^-}^{\text{org}}}{1 - x_{Q^+}^{\text{org}}} \\
\hat{x}_{QY}^{\text{org}} &= \frac{x_{Y^-}^{\text{org}}}{1 - x_{Q^+}^{\text{org}}} \\
\hat{x}_{RX}^{\text{org}} &= \frac{x_{RX}^{\text{org}}}{1 - x_{Q^+}^{\text{org}}} \\
\hat{x}_{RY}^{\text{org}} &= \frac{x_{RY}^{\text{org}}}{1 - x_{Q^+}^{\text{org}}} \\
\hat{x}_{I}^{\text{org}} &= \frac{x_{I}^{\text{org}}}{1 - x_{Q^+}^{\text{org}}}.
\end{aligned} \tag{4}
$$

With these relations, let us now move on to the model equations. We represent the LLPTC process of Figure 1a by the stirred cell model of Figure 1b. The aqueous stream of composition z^{aq} and molar flow rate F^{aq}, and the organic stream of composition z^{org} and molar flow rate F^{org}, form the input streams. The aqueous product stream of composition x^{aq} and molar flow rate P^{aq}, and the organic product stream of composition x^{org} and molar flow rate P^{org}, form the output streams. Both the aqueous and the organic phases are perfectly mixed except for thin stagnant films near the interface. The resistance to mass transfer is concentrated in these thin films and the mass transfer takes place through these films in the direction perpendicular to the interface.

Reaction kinetics

The rate of reaction per mole of the organic phase of composition $\hat{x}^{\text{org}}$ is written as

$$r(\hat{\boldsymbol{x}}^{\text{org}}) = k_f\left[\gamma_{RY}^{\text{org}}\hat{x}_{RY}^{\text{org}}\gamma_{QX}^{\text{org}}\hat{x}_{QX}^{\text{org}} - \frac{1}{K}\gamma_{RX}^{\text{org}}\hat{x}_{RX}^{\text{org}}\gamma_{QY}^{\text{org}}\hat{x}_{QY}^{\text{org}}\right], \quad (5)$$

where γ_i^{org} are liquid-phase activity coefficients based on appropriate standard states. In this article we will assume the organic phase to behave ideally ($\gamma_i^{\text{org}} = 1,\ \forall i$). Whenever thermodynamic models and parameters for activity coefficients are available, the nonideality can easily be considered. With this assumption, the above rate expression takes the form

$$r(\hat{\boldsymbol{x}}^{\text{org}}) = k_f\left[\hat{x}_{RY}^{\text{org}}\hat{x}_{QX}^{\text{org}} - \frac{1}{K}\hat{x}_{RX}^{\text{org}}\hat{x}_{QY}^{\text{org}}\right], \quad (6)$$

This expression can be written in terms of the apparent mole fractions as

$$r(\boldsymbol{x}^{\text{org}}) = \frac{k_f}{1 - x_{Q^\pm}^{\text{org}}}\left[x_{RY}^{\text{org}}x_{X^-}^{\text{org}} - \frac{1}{K}x_{RX}^{\text{org}}x_{Y^-}^{\text{org}}\right]. \quad (7)$$

In these equations, K is the equilibrium constant defined as

$$K = \frac{k_f}{k_r} = \left[\frac{x_{RX}^{\text{org}}x_{Y^-}^{\text{org}}}{x_{RY}^{\text{org}}x_{X^-}^{\text{org}}}\right]_{\text{eq}}. \quad (8)$$

The subscript eq indicates reaction equilibrium and k_f and k_r denote the forward and backward reaction rate constants, respectively.

Mass transfer

The molar fluxes at the interface relative to stationary coordinates can be written in terms of mass transfer coefficients ($K_{m_i}^{I\phi},\ \phi = \text{aq, org}$) as

$$\overline{N}_i^{I\phi} = \bar{J}_i^{I\phi} + x_i^{I\phi}\overline{N}_T^{I\phi} = -c_T^{\phi}K_{m_i}^{I\phi}\Delta x_i^{\phi} + x_i^{I\phi}\overline{N}_T^{I\phi},$$
$$i = Q^+,\ X^-,\ Y^-,\ M^+,\ RX,\ RY,\ W,\ I,$$
$$\phi = \text{aq, org}. \quad (9)$$

Overbars indicate directional quantities. Superscript I indicates quantities evaluated at the interface. $\overline{N}_T^{I\phi}$ is the total molar flux at the interface in phase ϕ. The composition difference driving forces are defined as

$$\Delta x_i^{\text{aq}} = x_i^{I\text{aq}} - x_i^{\text{aq}}$$
$$\Delta x_i^{\text{org}} = x_i^{\text{org}} - x_i^{I\text{org}}$$
$$i = Q^+,\ X^-,\ Y^-,\ M^+,\ RX,\ RY,\ W,\ I. \quad (10)$$

x_i^{aq} and x_i^{org} represent the bulk aqueous and organic-phase mole fractions. Note that the composition difference driving forces are directional quantities. However, they are not represented by overbars as the sense of direction is preserved in the above definition. This direction is assumed to be positive going from the aqueous phase into the organic phase.

Note that in Eq. 9 we have used the Fickian formulation for describing the mass transfer across the interface. A more generalized Maxwell-Stefan formulation can also be easily used, in which case the equations for fluxes at the interface will take the following form (repeated indices imply summation)

$$\overline{N}_i^{I\phi} = \bar{J}_i^{I\phi} + x_i^{I\phi}\overline{N}_T^{I\phi} = -c_T^{\phi}K_{m_{ij}}^{I\phi}\Delta x_j^{\phi} + x_i^{I\phi}\overline{N}_T^{I\phi},$$
$$i = Q^+,\ X^-,\ Y^-,\ M^+,\ RX,\ RY,\ W,\ I,$$
$$\phi = \text{aq, org}. \quad (11)$$

Here, the mass-transfer coefficient $K_{m_{ij}}^{I\phi}$ accounts for the transport of component i due to the gradient in composition of component j. The Fickian formulation is a special case of the generalized Maxwell-Stefan formulation in which the gradient in composition of component j has no effect on the transport of component i ($K_{m_{ij}}^{I\phi} = 0,\ i \neq j,\ K_{m_{ij}}^{I\phi} = K_{m_i}^{I\phi},\ i = j$). For phase-transfer catalyzed systems, data on the mass-transfer coefficients for the Maxwell-Stefan formulation are not readily available. Therefore, we use the Fickian formulation.

Bootstrap solution

The description of mass transfer given by Eqs. 9 and 10 is not complete as these equations are not closed (that is, we need to know $\overline{N}_T^{I\phi}$ to evaluate $\overline{N}_i^{I\phi}$ ($\forall i$) and $\overline{N}_i^{I\phi}$ ($\forall i$) to evaluate $\overline{N}_T^{I\phi}$). This bootstrap problem (Krishna and Taylor, 1986) is resolved as follows.

At the interface, the continuity of fluxes implies

$$\overline{N}_i^{I\text{aq}} = \overline{N}_i^{I\text{org}} = \overline{N}_i^{I},$$
$$i = Q^+, X^-, Y^-, M^+, RX, RY, W, I$$
$$\Rightarrow \quad \overline{N}_T^{I\text{aq}} = \overline{N}_T^{I\text{org}} = \overline{N}_T^{I}. \quad (12)$$

Using Eqs. 9 and 12, we can write the bootstrap solution as

$$\overline{N}_T^{I} = \frac{c_T^{\text{org}}K_{m_i}^{I\text{org}}\Delta x_i^{\text{org}} - c_T^{\text{aq}}K_{m_i}^{I\text{aq}}\Delta x_i^{\text{aq}}}{x_i^{I\text{org}} - x_i^{I\text{aq}}}$$
$$i = Q^+, X^-, Y^-, M^+, RX, RY, W, I. \quad (13)$$

With this solution, we can rewrite Eq. 9 as:

$$\overline{N}_i^{I} = \frac{x_i^{I\text{aq}}}{x_i^{I\text{org}} - x_i^{I\text{aq}}}c_T^{\text{org}}K_{m_i}^{I\text{org}}\Delta x_i^{\text{org}} + \frac{x_i^{I\text{org}}}{x_i^{I\text{aq}} - x_i^{I\text{org}}}c_T^{\text{aq}}K_{m_i}^{I\text{aq}}\Delta x_i^{\text{aq}},$$
$$i = Q^+, X^-, Y^-, M^+, RX, RY, W, I. \quad (14)$$

This equation, along with the phase equilibrium equations at the interface, completely describes the mass-transfer process. Let us now consider the phase equilibrium at the interface.

Phase equilibrium

The only components that move across the interface of the stirred cell are salts QX and QY. As noted earlier, these salts dissociate completely in the aqueous phase and exist as ion-pairs in the organic phase. At the interface, at equilibrium, the chemical potential of the ion pair in the organic phase should be equal to the sum of the chemical potentials of its constituent ions in the aqueous phase

$$(\mu_{QX})^{I\text{org}} = (\mu_{Q^+})^{I\text{aq}} + (\mu_{X^-})^{I\text{aq}}$$
$$(\mu_{QY})^{I\text{org}} = (\mu_{Q^+})^{I\text{aq}} + (\mu_{Y^-})^{I\text{aq}}. \quad (15)$$

The chemical potentials of the ions are defined as (for example, for Q^+)

$$\mu_{Q^+} = \mu^*_{Q^+} + RT \ln\left(\gamma^*_{Q^+}[Q^+]\right). \quad (16)$$

Superscript $*$ indicates that infinite dilution standard state (asymmetric normalization) is used and the activity coefficients are based on molal compositions (Pitzer, 1995). The chemical potentials of the ion-pairs are similarly defined as (for example, for QX)

$$\mu_{QX} = \mu^*_{QX} + RT \ln\left(\gamma^*_{QX}[QX]\right). \quad (17)$$

Here again the infinite dilution standard state is used and the activity coefficients are based on molal compositions. Using these definitions and assuming ideal behavior, the phase equilibrium equations can be rewritten as

$$\frac{[QX]^{I\text{org}}}{[Q^+]^{I\text{aq}}[X^-]^{I\text{aq}}} = \exp\left\{\frac{1}{RT}\left[(\mu^*_{Q^+} + \mu^*_{X^-})^{I\text{aq}} - (\mu^*_{QX})^{I\text{org}}\right]\right\} = E^*_{QX}$$

$$\frac{[QY]^{I\text{org}}}{[Q^+]^{I\text{aq}}[Y^-]^{I\text{aq}}} = \exp\left\{\frac{1}{RT}\left[(\mu^*_{Q^+} + \mu^*_{Y^-})^{I\text{aq}} - (\mu^*_{QY})^{I\text{org}}\right]\right\} = E^*_{QY}. \quad (18)$$

E^*_{QX} and E^*_{QY} are functions only of temperature. They can be rewritten in terms of mole fractions as

$$E_{QX} = E^*_{QX}\frac{M_I}{(M_W)^2} = \frac{x^{I\text{org}}_{X^-}\left(x^{I\text{aq}}_W\right)^2}{x^{I\text{org}}_I x^{I\text{aq}}_{Q^+} x^{I\text{aq}}_X}$$

$$E_{QY} = E^*_{QY}\frac{M_I}{(M_W)^2} = \frac{x^{I\text{org}}_{Y^-}\left(x^{I\text{aq}}_W\right)^2}{x^{I\text{org}}_I x^{I\text{aq}}_{Q^+} x^{I\text{aq}}_{Y^-}}. \quad (19)$$

E_{QX} and E_{QY} determine how QX and QY are distributed at the aqueous-organic interface at phase equilibrium. Therefore, they are known as the equilibrium distribution coefficients for QX and QY, respectively. Our analysis reveals that when derived as above, they are constant at constant temperature. Data for the distribution coefficients can be obtained by using data for the standard state chemical potentials from suitable thermodynamic tables.

Conservation equations

The set of linearly independent material balance equations for the stirred cell representing the LLPTC process can be written as

$$P^{\text{aq}} = F^{\text{aq}} - a\overline{N}^I_T$$
$$P^{\text{aq}}x^{\text{aq}}_i = F^{\text{aq}}z^{\text{aq}}_i - a\overline{N}^I_i, \qquad i = Q^+, X^-, Y^-$$
$$P^{\text{org}} = F^{\text{org}} + a\overline{N}^I_T$$
$$P^{\text{org}}x^{\text{org}}_i = F^{\text{org}}z^{\text{org}}_i + H^{\text{org}}\upsilon_i r(\boldsymbol{x}^{\text{org}}) + a\overline{N}^I_i, \qquad i = Q^+, X^-, RX, RY \quad (20)$$

Note that in choosing the above linearly independent equations, we have used the fact that

$$z^{\text{org}}_W = z^{\text{org}}_{M^+} = z^{\text{aq}}_{RX} = z^{\text{aq}}_{RY} = z^{\text{aq}}_I = 0 \quad (21a)$$
$$x^{\text{org}}_{M^+} = x^{I\text{org}}_{M^+} = x^{\text{org}}_W = x^{I\text{org}}_W = 0 \quad (21b)$$
$$x^{\text{aq}}_{RX} = x^{I\text{aq}}_{RX} = x^{\text{aq}}_{RY} = x^{I\text{aq}}_{RY} = x^{\text{aq}}_I = x^{I\text{aq}}_I = 0 \quad (21c)$$

and the condition of electroneutrality

$$z^{\text{aq}}_{Q^+} + z^{\text{aq}}_{M^+} = z^{\text{aq}}_{X^-} + z^{\text{aq}}_{Y^-}$$
$$x^{\text{aq}}_{Q^+} + x^{\text{aq}}_{M^+} = x^{\text{aq}}_{X^-} + x^{\text{aq}}_{Y^-}$$
$$x^{I\text{aq}}_{Q^+} + x^{I\text{aq}}_{M^+} = x^{I\text{aq}}_{X^-} + x^{I\text{aq}}_{Y^-}$$
$$z^{\text{org}}_{Q^+} = z^{\text{org}}_{X^-} + z^{\text{org}}_{Y^-}$$
$$x^{\text{org}}_{Q^+} = x^{\text{org}}_{X^-} + x^{\text{org}}_{Y^-}$$
$$x^{I\text{org}}_{Q^+} = x^{I\text{org}}_{X^-} + x^{I\text{org}}_{Y^-} \quad (22)$$

We have also assumed that the molar holdups in the films in each phase are negligible in comparison to the total molar holdup in the bulk of each phase. Hence, the compositions of the aqueous and the organic product streams are the same as the bulk compositions of the aqueous and the organic phases, respectively. This assumption is generally valid for all types of industrial liquid-liquid contactors. Dividing Eq. 20 by ($F = F^{\text{aq}} + F^{\text{org}}$) and using the constitutive equations for reaction kinetics and mass transfer, we get

$$\frac{P^{\text{aq}}}{F} = \frac{F^{\text{aq}}}{F} - \frac{Da^{\text{org}}_{m_{Q^+}}\Delta x^{\text{org}}_{Q^+} - Da^{\text{aq}}_{m_{Q^+}}\Delta x^{\text{aq}}_{Q^+}}{x^{I\text{org}}_{Q^+} - x^{I\text{aq}}_{Q^+}} \quad (23a)$$

$$\frac{P^{\text{aq}}}{F}x^{\text{aq}}_i = \frac{F^{\text{aq}}}{F}z^{\text{aq}}_i - \frac{x^{I\text{aq}}_i}{x^{I\text{org}}_i - x^{I\text{aq}}_i}Da^{\text{org}}_{m_i}\Delta x^{\text{org}}_i - \frac{x^{I\text{org}}_i}{x^{I\text{aq}}_i - x^{I\text{org}}_i}Da^{\text{aq}}_{m_i}\Delta x^{\text{aq}}_i, \quad (23b)$$

$$i = Q^+, X^-, Y^-$$

$$\frac{P^{\text{org}}}{F} = \frac{F^{\text{org}}}{F} + \frac{Da^{\text{org}}_{m_{Q^+}} \Delta x^{\text{org}}_{Q^+} - Da^{\text{aq}}_{m_{Q^+}} \Delta x^{\text{aq}}_{Q^+}}{x^{I\text{org}}_{Q^+} - x^{I\text{aq}}_{Q^+}} \tag{23c}$$

$$\frac{P^{\text{org}}}{F} x^{\text{org}}_i = \frac{F^{\text{org}}}{F} z^{\text{org}}_i + Da^{\text{org}}_r \upsilon_i \frac{r(\boldsymbol{x}^{\text{org}})}{k_f} + \frac{x^{I\text{aq}}_i}{x^{I\text{org}}_i - x^{I\text{aq}}_i} Da^{\text{org}}_{m_i} \Delta x^{\text{org}}_i + \frac{x^{I\text{org}}_i}{x^{I\text{aq}}_i - x^{I\text{org}}_i} Da^{\text{aq}}_{m_i} \Delta x^{\text{aq}}_i,$$

$$i = Q^+, X^-, RX, RY \tag{23d}$$

Here, the dimensionless Damköhler numbers for reaction (Da^{org}_r) and mass transfer ($Da^{\text{aq}}_{m_i}$, $Da^{\text{org}}_{m_i}$) are defined as

$$Da^{\text{org}}_r = \frac{H^{\text{org}}/F}{1/k_f}$$

$$Da^{\phi}_{m_i} = \frac{H^{\phi}/F}{H^{\phi}/ac^{\phi}_T K^{I\phi}_{m_i}}, \qquad \forall i, \quad \phi = \text{aq, org} \tag{24}$$

The Damköhler number for reaction compares the characteristic residence time of the organic phase to the characteristic time for the organic-phase reaction. Similarly, the Damköhler numbers for mass transfer in aqueous and organic phases compare the characteristic residence time of the respective phase to the characteristic time for mass transfer in that phase.

In Eqs. 23a and 23c, $\overline{N}^I_T$ was evaluated by using Eq. 13 for component Q^+. We could have equivalently used any other component in its place. Therefore, our model has to satisfy the following five additional equations (only five such equations are linearly independent)

$$\frac{c^{\text{org}}_T K^{I\text{org}}_{m_i} \Delta x^{\text{org}}_i - c^{\text{aq}}_T K^{I\text{aq}}_{m_i} \Delta x^{\text{aq}}_i}{x^{I\text{org}}_i - x^{I\text{aq}}_i} = \frac{c^{\text{org}}_T K^{I\text{org}}_{m_{Q^+}} \Delta x^{\text{org}}_{Q^+} - c^{\text{aq}}_T K^{I\text{aq}}_{m_{Q^+}} \Delta x^{\text{aq}}_{Q^+}}{x^{I\text{org}}_{Q^+} - x^{I\text{aq}}_{Q^+}},$$

$$i = X^-, Y^-, RX, RY, W. \tag{25}$$

Also, the mole fractions of the inlet streams, the mole fractions in the bulk phases, and the mole fractions at the interface add up to unity

$$\sum_i z^{\text{org}}_i = \sum_i z^{\text{aq}}_i = \sum_i x^{\text{org}}_i = \sum_i x^{\text{aq}}_i = \sum_i x^{I\text{org}}_i = \sum_i x^{I\text{aq}}_i = 1. \tag{26}$$

Degrees of freedom

Let us now determine the number of independent variables for the model. We have nine independent material balance equations (Eqs. 23a to 23d), two phase equilibrium equations at the interface (Eq. 19), six equations given by the condition of electroneutrality (Eq. 22), five constraints given by Eq. 25, and six equations given by Eq. 26; hence, a total of 28 equations. These equations contain the following 52 variables: F^{aq}, F^{org}, P^{aq}, P^{org}, $\boldsymbol{z}^{\text{aq}}$, $\boldsymbol{z}^{\text{org}}$, $\boldsymbol{x}^{\text{aq}}$, $\boldsymbol{x}^{\text{org}}$, $\boldsymbol{x}^{I\text{aq}}$, and $\boldsymbol{x}^{I\text{org}}$. Therefore, we have 24 degrees of freedom. These are completely specified by fixing the following 14 variables: F^{aq}, F^{org}, z^{aq}_i, $i = Q^+, X^-, Y^-, RX, RY, W$, and z^{org}_i, $i = Q^+, X^-, Y^-, RX, RY, W$ (two remaining mole fractions of the aqueous and organic feedstreams can be evaluated by using Eqs. 22 and 26 and, hence, need not be specified) and by using the 10 conditions of Eqs. 21b and 21c. Thus, for given molar flow rates and compositions of the aqueous and organic input streams, the performance of a LLPTC process can be completely characterized by the dimensionless Damköhler numbers and the thermodynamic parameters (K, E_{QX}, and E_{QY}).

This completes the development of the mathematical model for the LLPTC processes. Let us now study some important insights that we can obtain from this model.

Table 1. Specifications for the Example System

Aqueous Feed	Organic Feed
$F^{\text{aq}} = 6.28$	$F^{\text{org}} = 1.0$
$z^{\text{aq}}_{q^+} = 0.0$	$z^{\text{org}}_{Q^+} = 0.00527$
$z^{\text{aq}}_{X^-} = 0.0336$	$z^{\text{org}}_{X^-} = 0.0$
$z^{\text{aq}}_{Y^-} = 0.0$	$z^{\text{org}}_{Y^-} = 0.00527$
$z^{\text{aq}}_{M^+} = 0.0336$	$z^{\text{org}}_{RX} = 0.0$
$z^{\text{aq}}_W = 0.9328$	$z^{\text{org}}_{RY} = 0.0527$
	$z^{\text{org}}_I = 0.93676$
Base-Case Values of Thermodynamic Parameters	
$K = 1$	
$E_{QX} = 1{,}000$	
$E_{QY} = 10$	

Effect of Kinetics and Mass Transfer

To understand the effect of kinetics and mass transfer, let us consider a LLPTC stirred cell with the input flow rates and compositions as listed in Table 1. These input specifications are similar to the example of conversion of bromooctane to iodooctane with chlorobenzene as the organic solvent and tetrabutylammonium bromide as the PT catalyst (Stanley and Quinn, 1987). Base-case thermodynamic parameters are also listed in Table 1. Let us now explore how the rates of reaction and mass transfer, relative to each other and relative to the rate of product removal, govern the aqueous- and organic-phase compositions of the stirred cell.

Departure from reaction equilibrium

Figure 2 shows the departure from reaction equilibrium of the bulk organic-phase composition as a function of $Da^{\text{org}}_r/Da^{\text{org}}_m$. This departure function is defined as

$$\text{Departure from reaction equilibrium} = \frac{x^{\text{org}}_{RX} x^{\text{org}}_{Y^-}}{K x^{\text{org}}_{RY} x^{\text{org}}_{X^-}}. \tag{27}$$

It is assumed that the mass-transfer coefficients of all components are the same ($Da^{\phi}_{m_i} = Da^{\phi}_m$, $\forall i$, $\phi = \text{aq, org}$) and Da^{aq}_m is high ($= 100$). The ratio $Da^{\text{org}}_r/Da^{\text{org}}_m$ compares the rate of the organic-phase reaction to the rate of mass transfer into

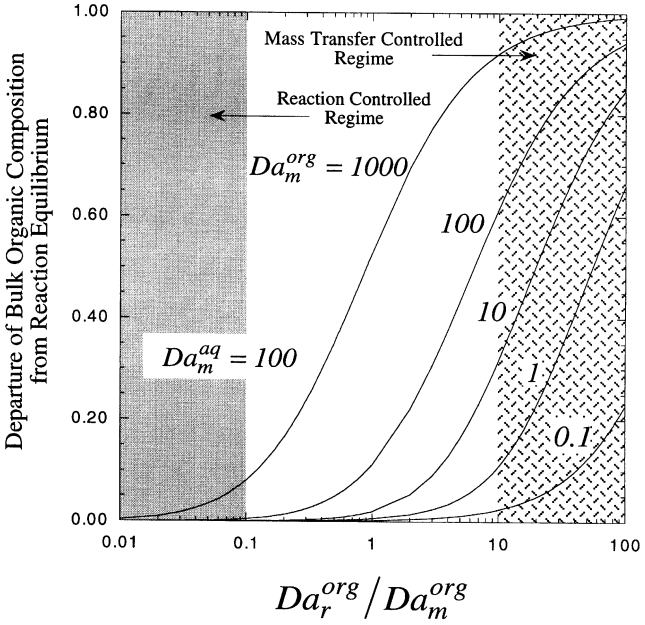

Figure 2. Departure of the bulk organic phase composition from reaction equilibrium.

the organic phase. It is, in principle, similar to the Hatta number.

High values of Da_r^{org}/Da_m^{org} represent the mass-transfer controlled regime, in which the reaction is much faster than the mass transfer across the interface. The reaction takes place essentially in the film near the interface and the bulk organic phase is in reaction equilibrium. Low values of Da_r^{org}/Da_m^{org} represent the reaction controlled regime. In this regime, the reaction is much slower than the mass transfer. As the reaction takes place both in the film as well as in the bulk organic phase, the bulk composition shows significant departure from reaction equilibrium. The reaction controlled regime and the mass-transfer controlled regime are indicated in Figure 2 as a uniformly shaded region and a patterned region, respectively. The same convention is followed throughout this article. Note that the boundaries of these regimes are not sharp.

The performance of the stirred cell depends not only on the relative rates of reaction and mass transfer, but also on their rates relative to the rate of product removal. Therefore, the departure from reaction equilibrium becomes more pronounced as the value of Da_m^{org} decreases (that is, as both reaction and mass transfer become progressively slower than product removal).

Departure from phase equilibrium

Figures 3 and 4 show the departure from phase equilibrium of the bulk aqueous and organic phase compositions, respectively. These departure functions are defined as

Departure of aqueous Q^+, X^- composition

$$= \frac{x_{X^-}^{I\text{org}} \left(x_W^{\text{aq}}\right)^2}{E_{QX} x_I^{I\text{org}} x_{Q^+}^{\text{aq}} x_{X^-}^{\text{aq}}}, \qquad (28a)$$

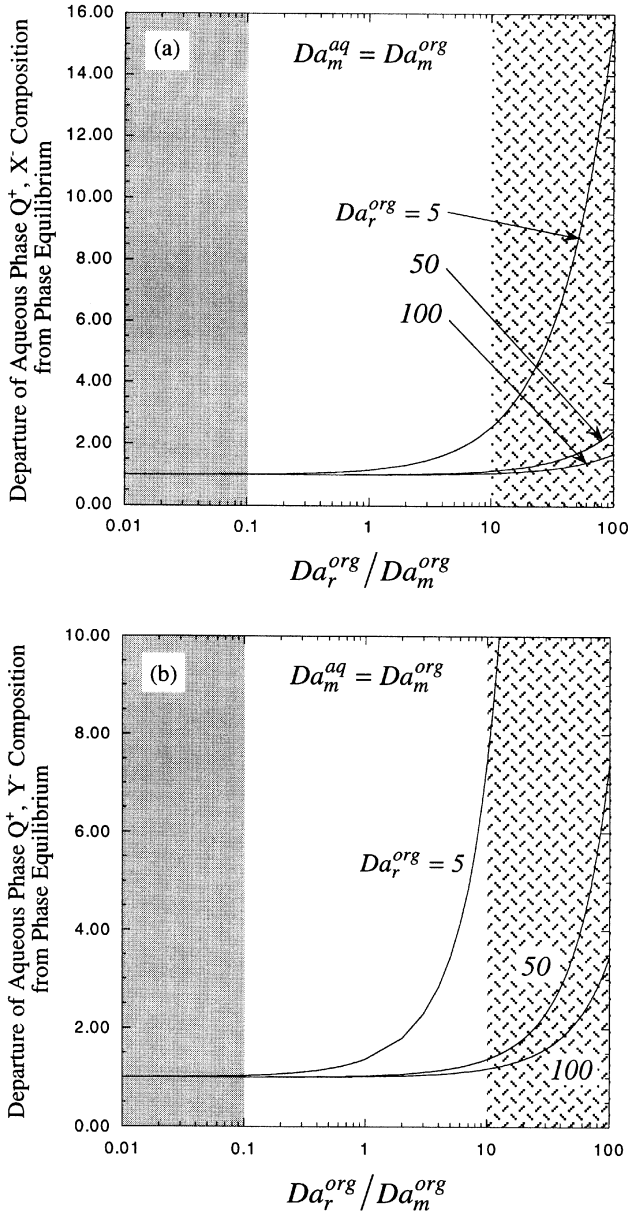

Figure 3. Departure of the bulk aqueous phase composition from phase equilibrium.

(a) Q^+, X^- composition; (b) Q^+, Y^- composition.

Departure of aqueous Q^+, Y^- composition

$$= \frac{x_{Y^-}^{I\text{org}} \left(x_W^{\text{aq}}\right)^2}{E_{QY} x_I^{I\text{org}} x_{Q^+}^{\text{aq}} x_{Y^-}^{\text{aq}}}, \qquad (28b)$$

Departure of organic QX composition

$$= \frac{x_{X^-}^{\text{org}} \left(x_W^{I\text{aq}}\right)^2}{E_{QX} x_I^{\text{org}} x_{Q^+}^{I\text{aq}} x_{X^-}^{I\text{aq}}}, \qquad (28c)$$

Departure of organic QY composition

$$= \frac{x_{Y^-}^{\text{org}} \left(x_W^{I\text{aq}}\right)^2}{E_{QY} x_I^{\text{org}} x_{Q^+}^{I\text{aq}} x_{Y^-}^{I\text{aq}}}. \qquad (28d)$$

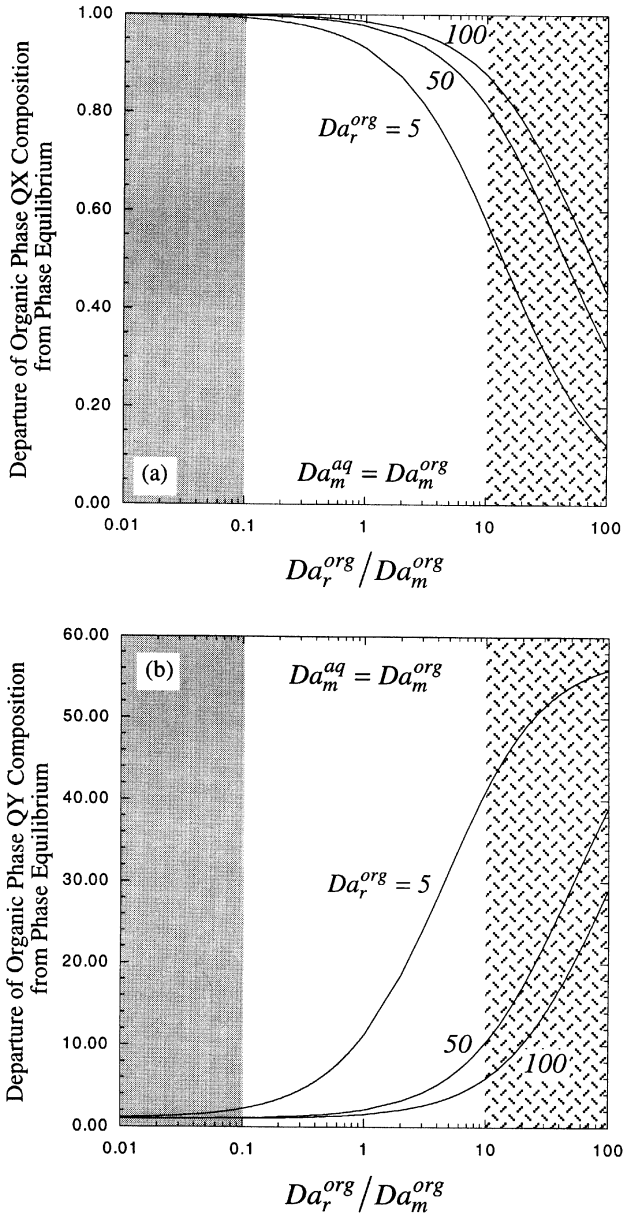

Figure 4. Departure of the bulk organic phase composition from phase equilibrium.

(a) QX composition; (b) QY composition.

Here again, it is assumed that the Damköhler numbers for the mass transfer of all components in both phases are the same ($Da_{m_i}^{\phi} = Da_m^{\phi}$, $\forall i$, $\phi = \text{aq, org}$ and $Da_m^{\text{org}} = Da_m^{\text{aq}}$). As expected, in the reaction controlled regime, the bulk compositions of both phases are in phase equilibrium (deviations close to unity). Here, mass transfer across the interface is much faster than the organic-phase reaction and, therefore, composition gradients in both phases are negligible (bulk compositions are almost the same as the interface compositions). As we move towards the mass-transfer controlled regime, these gradients start to become more and more significant. As a result, the bulk compositions of both phases differ considerably from their respective interface compositions (which are always in phase equilibrium). This results in the departures of the bulk organic- and aqueous-phase compositions from phase equilibrium becoming more and more significant, as we move from the reaction controlled regime to the mass-transfer controlled regime. Also, note that the deviations become more pronounced as Da_r^{org} decreases (that is, as both reaction and mass transfer become slower than product removal).

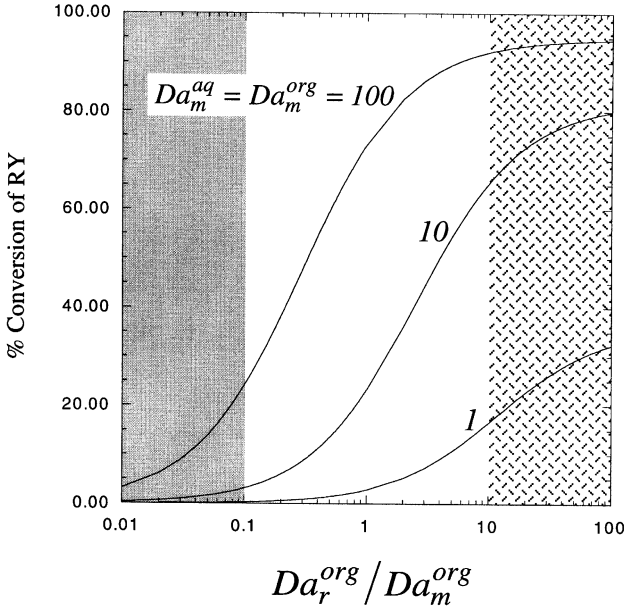

Figure 5. Performance in various operating regimes.

From these results, we can conclude that in the limit of infinitely high Damköhler numbers, both phases are in phase equilibrium and the organic phase is in reaction equilibrium. This corresponds to the thermodynamic limit of the system. We will study this thermodynamic limit in more detail later on. Before we do so, let us now see how the performance of the stirred cell is affected by the rate processes.

Effect of kinetics and mass transfer on conversion

The effect of kinetics and mass transfer on the performance of the stirred cell for the given process is shown in Figure 5. The performance is characterized by the conversion of the organic reactant RY

$$\text{Conversion} = X = 1 - \frac{P^{\text{org}} x_{RY}^{\text{org}}}{F^{\text{org}} z_{RY}^{\text{org}}} = \frac{P^{\text{org}} x_{RX}^{\text{org}}}{F^{\text{org}} z_{RY}^{\text{org}}}. \qquad (29)$$

Here again, we have assumed that $Da_{m_i}^{\phi} = Da_m^{\phi}$, $\forall i$, $\phi = \text{aq, org}$, and $Da_m^{\text{org}} = Da_m^{\text{aq}}$. Figure 5 indicates that the conversion increases as we go from the reaction controlled regime to the mass-transfer controlled regime. We can also see that the conversion is higher for higher values of $Da_m^{\text{org,aq}}$. For this system, the highest value of conversion, and, therefore, the best performance, is obtained at the thermodynamic limit. This is generally true for all LLPTC systems with a single organic-phase reaction. For multiple organic phase reactions, a tradeoff may exist between conversion and selectivity.

Thermodynamic Limit

At the thermodynamic limit, all the Damköhler numbers are infinitely high. Composition gradients do not exist in both phases as there is no resistance to mass transfer. Also, the organic phase is in reaction equilibrium and in phase equilibrium with the aqueous phase. The conservation equations, when modified accordingly, have zero degrees of freedom for specified feed flow rates and compositions. Therefore, the system has a unique value of conversion for the given values of the thermodynamic parameters. From the definitions of K, E_{QX}, E_{QY}, and X, we can write (by omitting subscript eq and superscript I for convenience)

$$X = \frac{K\dfrac{E_{QX}}{E_{QY}}}{K\dfrac{E_{QX}}{E_{QY}} + \dfrac{x^{aq}_{Y^-}}{x^{aq}_{X^-}}}. \tag{30}$$

With this equation, let us now study the effect of varying the thermodynamic parameters on the performance of the stirred cell in the thermodynamic limit. Recall that the results presented in the previous section were obtained for the base-case values of the thermodynamic parameters ($K = 1$, $E_{QX} =$ 1,000, and $E_{QY} = 10$).

Effect of reaction equilibrium constant

The reaction equilibrium constant K can vary from 0 (no reaction limit) to ∞ (irreversible reaction limit). From Eq. 30, we get

$$\lim_{K \to 0} X = 0, \tag{31a}$$

$$\lim_{K \to \infty} X = 1. \tag{31b}$$

In the no reaction limit, the conversion is obviously zero. In the irreversible reaction limit, the organic reactant is fully converted at equilibrium. This is also obvious as the thermodynamic limit corresponds to infinitely large residence times for both phases in the stirred cell. For intermediate values of K, the conversion increases from 0 to 1 as we go from the no reaction limit to the irreversible reaction limit. This is shown in Figure 6, which is calculated by solving the modified conservation equations. The results also show that for a fixed value of K, the conversion is higher for higher values of the ratio E_{QX}/E_{QY}. The equilibrium distribution coefficients E_{QX} and E_{QY} are measures of the organophilicity of the ion-pairs QX and QY, respectively. The higher the organophilicity of QX and QY, the higher the values of E_{QX} and E_{QY}. Note that the ion-pair QX is a reactant and the ion-pair QY is a product of the organic-phase reaction. Therefore, we get better conversion as the organophilicity of QX increases with respect to the organophilicity of QY (that is, for higher values of E_{QX}/E_{QY}). The difference, however, is not very significant for very low and very high values of K as the conversion is very close to 0 and to 1, respectively.

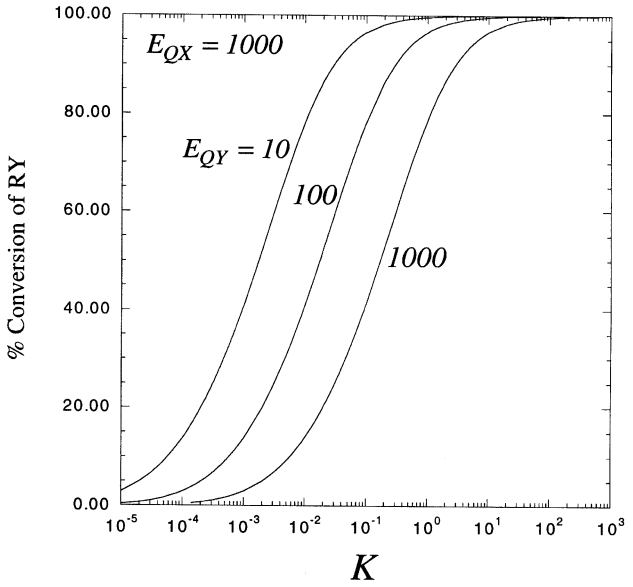

Figure 6. Performance at thermodynamic equilibrium.
Effect of the reaction equilibrium constant.

Effect of equilibrium distribution coefficients

Figures 7 and 8 show how the performance of the stirred cell varies with the equilibrium distribution coefficients E_{QX} and E_{QY}. From Eq. 30, we have

$$\lim_{\frac{E_{QX}}{E_{QY}} \to 0} X = 0, \tag{32a}$$

$$\lim_{\frac{E_{QX}}{E_{QY}} \to \infty} X = 1. \tag{32b}$$

Figure 7a shows the variation of conversion with the ratio E_{QX}/E_{QY} for a low value of K ($= 0.1$) and a low ($= 1$) and a high ($= 1{,}000$) value of E_{QX}. Figure 7b shows the corresponding variation of the ratio $x^{aq}_{Y^-}/x^{aq}_{X^-}$ (which appears in the denominator of Eq. 30). From this figure, we can observe that for a fixed value of E_{QX}/E_{QY}, $x^{aq}_{Y^-}/x^{aq}_{X^-}$ is different for different values of E_{QX} (and hence E_{QY}). Therefore, we would expect the conversion to depend not only on the ratio E_{QX}/E_{QY}, but also on the individual values of E_{QX} and E_{QY}. However, the results of Figure 7a indicate that the conversion changes only marginally with the individual values of E_{QX} (and, hence, E_{QY}) for a fixed E_{QX}/E_{QY}. Let us try to explain why.

For very low values of E_{QX}/E_{QY}, the individual values of E_{QX} and E_{QY} are not very significant as the conversion is very close to zero (Eq. 32a). Similarly, for higher values of the ratio, the individual values do not have a significant effect on conversion as $K(E_{QX}/E_{QY}) \gg x^{aq}_{Y^-}/x^{aq}_{X^-}$ and the conversion tends to unity (Eq. 32b). For intermediate values of E_{QX}/E_{QY}, $x^{aq}_{Y^-}/x^{aq}_{X^-}$ does not change appreciably with changing values of E_{QX} (and, hence, E_{QY}) as shown in Figure 7b. Therefore, in this case too, the conversion remains practically unchanged. For higher values of E_{QX} (and, hence, E_{QY}), slightly better conversion is obtained.

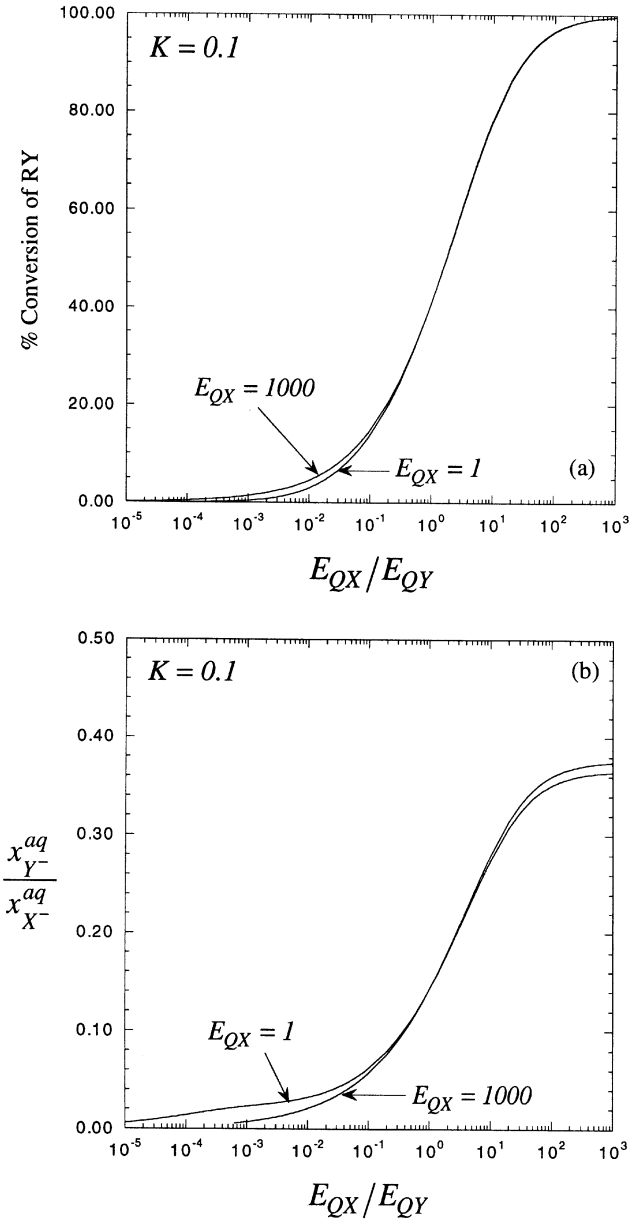

Figure 7. Performance at thermodynamic equilibrium.

Effect of the equilibrium distribution coefficients for K = 0.1.

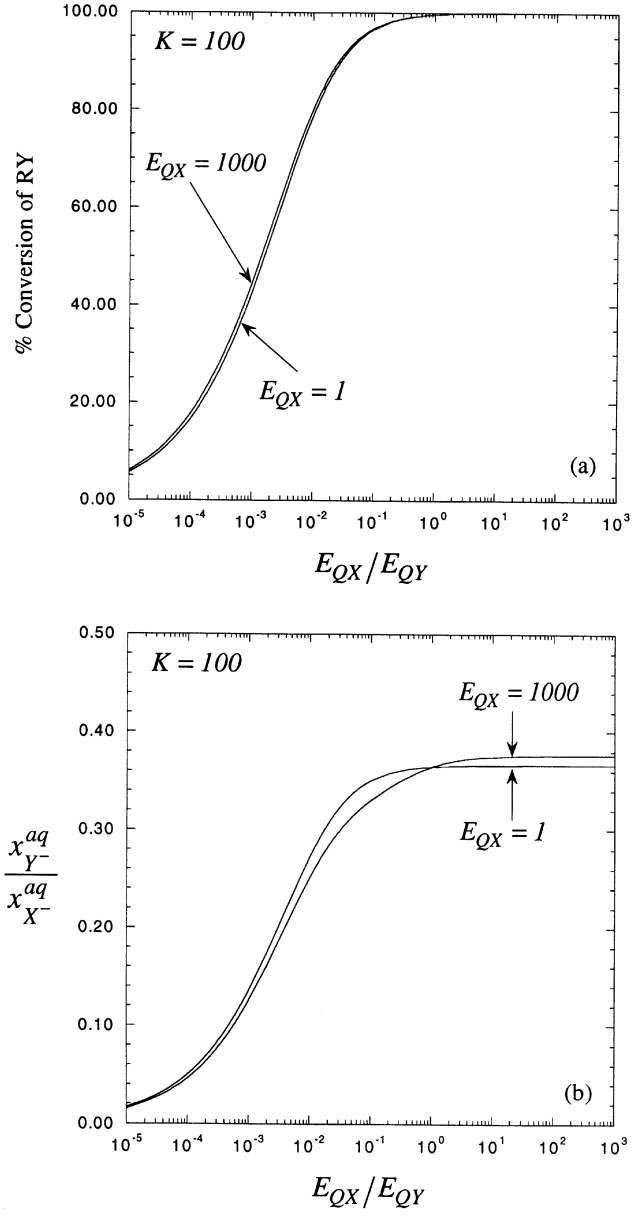

Figure 8. Performance at thermodynamic equilibrium.

Effect of the equilibrium distribution coefficients for K = 100.0.

Figures 8a and 8b show the similar variations of conversion and $x^{aq}_{Y^-}/x^{aq}_{X^-}$ with E_{QX}/E_{QY} for a high value of K (= 100). Similar observations can be made from these figures. Note that the conversion for any value of E_{QX} (and, hence, E_{QY}) is higher than the previous case as the reaction equilibrium constant is higher. In addition, the difference in conversions for the low (= 1) and for the high (= 1,000) values of E_{QX} is less than the previous case for intermediate values of E_{QX}/E_{QY}.

So far, we have seen that the best performance from the LLPTC stirred cell is obtained in the thermodynamic limit (very high values of the Damköhler numbers). We have also seen that the performance in the thermodynamic limit is influenced mainly by K and the ratio E_{QX}/E_{QY}. The best performance is obtained for irreversible reactions ($K \to \infty$) and for high values of E_{QX}/E_{QY}. The individual values of E_{QX} and E_{QY} do not significantly impact the conversion in the thermodynamic limit. Let us now study a few additional interesting aspects of the LLPTC process.

Additional Observations

Effect of equilibrium distribution coefficients on conversion away from thermodynamic limit

Figure 9 shows the conversion of RY as a function of the Damköhler numbers for various values of the equilibrium

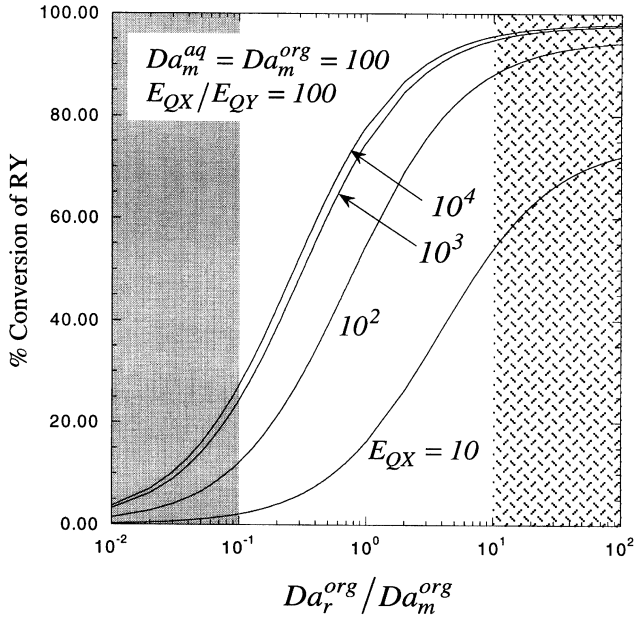

Figure 9. Effect of the equilibrium distribution coefficients on conversion away from the thermodynamic limit.

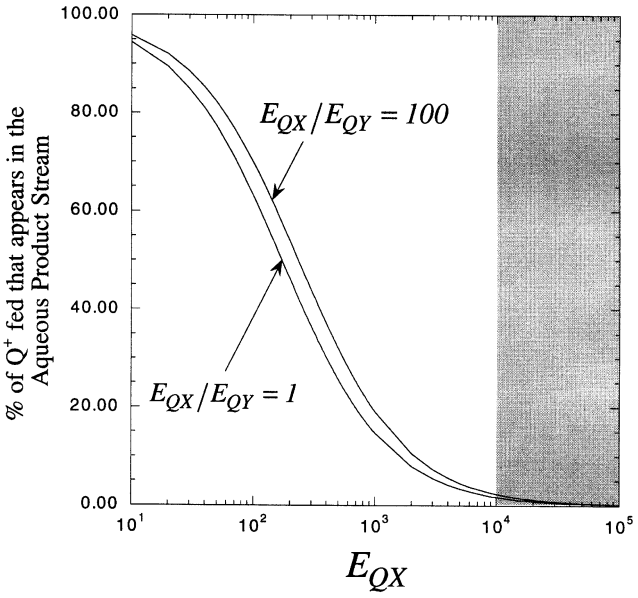

Figure 10. Performance at thermodynamic equilibrium: mechanistic aspect.

distribution coefficients. As seen before (Figure 5), the conversion increases as we go from the reaction controlled regime to the mass-transfer controlled regime. We have seen that the performance in the thermodynamic limit is insensitive to the individual values of E_{QX} and E_{QY} (Figures 7a and 8a). However, as we can see from Figure 9, the performance is dependent on the individual values of E_{QX} and E_{QY} for finite values of the Damköhler numbers. For a specified value of E_{QX}/E_{QY}, better conversion is obtained as the organophilicity of the ion pairs QX and QY increases (that is, as the individual values of E_{QX} and E_{QY} increase). Therefore, for industrial operation (finite values of the Damköhler numbers), it is necessary to not only have high values of E_{QX}/E_{QY}, but to also have high values of E_{QX} (and, hence, E_{QY}).

Mechanistic aspect

The LLPTC mechanism depicted in Figure 1a is known as the *extraction mechanism* due to Starks (1971). In this mechanism, the catalytic cation Q^+ is transported as an ion-pair from the aqueous phase to the organic phase and back, along with an appropriate anion (X^- or Y^-). In Figure 10 we have plotted the amount of Q^+ fed to the stirred cell that appears in the aqueous product stream at thermodynamic equilibrium as a function of the equilibrium distribution coefficients. This amount corresponds to

$$\frac{P^{\text{aq}} x_{Q^+}^{\text{aq}}}{F^{\text{org}} z_{Q^+}^{\text{org}} + F^{\text{aq}} z_{Q^+}^{\text{aq}}} \tag{33}$$

Note that the catalytic cation Q^+ is not consumed in the reaction. Therefore, the remaining moles of Q^+ appear in the organic product stream. For low values of E_{QX} and E_{QY}, most of Q^+ resides in the aqueous phase. In this case all three ions, Q^+, X^-, and Y^- are transferred across the interface as per Starks extraction mechanism. However, as the values of E_{QX} and E_{QY} increase, more and more of the Q^+ stays in the organic phase. For very high values of E_{QX} and E_{QY} (shaded region on the figure), the catalytic cation remains almost exclusively in the organic phase. In this situation, only the anions X^- and Y^- are transferred across the interface. This mechanism is conceptually similar to the *interface mechanism* proposed by Brändström and Montanari (Brändström, 1977). Therefore, it is not necessary to develop a separate model for the interfacial mechanism.

Effect of phase holdups

We have assumed the bulk organic and aqueous phases of the stirred cell to be perfectly mixed. Therefore, we can write

$$\frac{H^{\text{aq}}}{H^{\text{org}}} = \frac{F^{\text{aq}}}{F^{\text{org}}} \tag{34}$$

Therefore, the effect of changing the aqueous and the organic-phase holdups relative to each other can be studied by varying the ratio $F^{\text{aq}}/F^{\text{org}}$. The results are shown in Figure 11 (base-case values of the thermodynamic parameters are used). As the molar flow rate (or holdup) of the aqueous phase decreases, the number of moles of the cation X^- fed to the system decreases. Therefore, as expected, the conversion in the thermodynamic limit decreases; it is zero in the limit of no aqueous-phase feed. As we will discuss later, this result is useful in choosing the dispersed and continuous phases for a LLPTC reactor (Table 3).

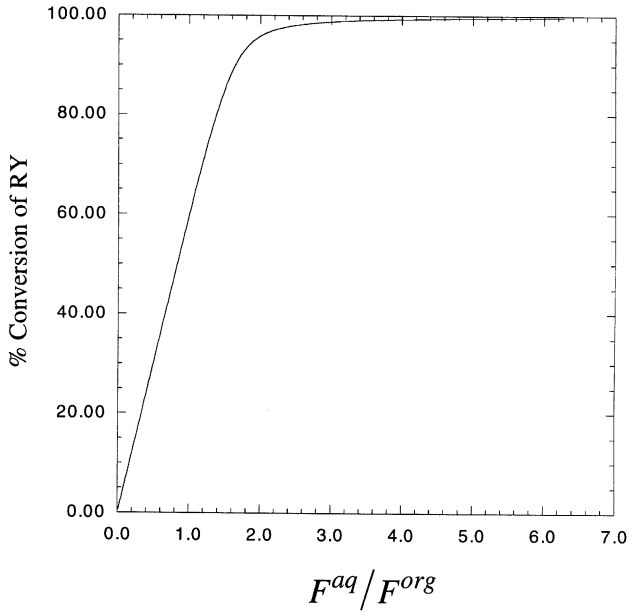

Figure 11. Effect of phase holdups.

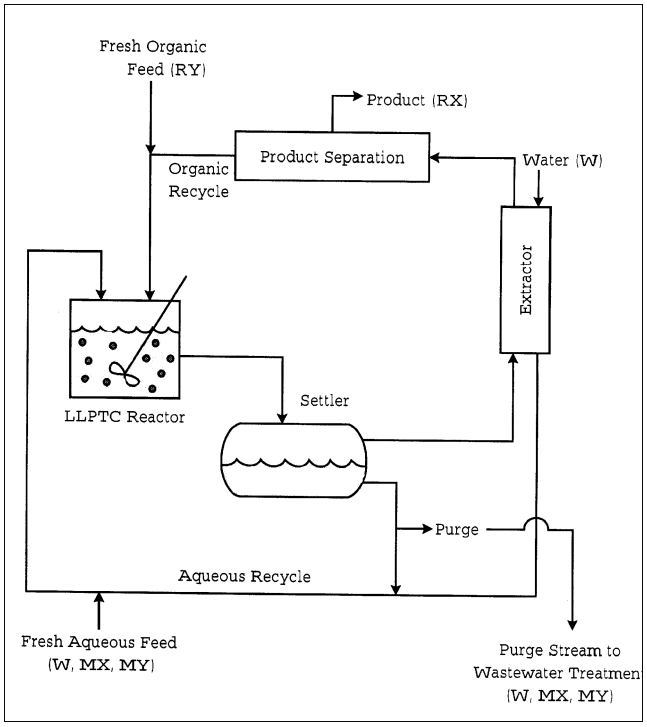

Figure 12. Class I flowsheet for a LLPTC process with catalyst recovery and recycle.

Catalyst recovery aspects

The key to successful industrial application of LLPTC processes is catalyst recovery and recycle. Catalyst recovery and recycle is crucial not only from an economic perspective, but also from an environmental perspective. However, it has unfortunately received very limited attention. Publications dealing with catalyst recovery aspects are very few and limited to the patent literature that deals with a few specific systems. This inadequacy has been stressed by Starks et al. (1994) and by Naik and Doraiswamy (1998). Here, we will attempt to fill in this gap by studying some catalyst recovery aspects on the basis of the stirred cell model.

We have developed two generic classes of flowsheets for LLPTC processes with catalyst recovery and recycle. These flowsheets are shown in Figures 12 to 14 and are developed on the basis of information collected from the patent literature (Masuko et al., 1979; Berris, 1991; Reed and Snedecor, 1995; Johnson, 1996, 1997) to cite a few. The important point of distinction between the two classes is that in Class I, the catalyst is separated before the product, whereas in Class II, the product is separated before the catalyst. First, let us briefly go through these flowsheets.

In the Class I flowsheet (Figure 12), the aqueous and organic phases are separated in the settler that follows the stirred-tank LLPTC reactor. The organic phase contains most of the catalyst. The catalyst is removed from the organic phase by washing it with water in a countercurrent (or crosscurrent) extractor. The aqueous stream from the extractor is recycled back to the LLPTC reactor. The organic stream from the extractor, which is now almost free of the catalyst, is then sent to the product separation unit. This is very often a distillation column (or a series of columns) that separates the product from the organic solvent and the unconverted reactant, which are recycled back to the LLPTC reactor. The aqueous phase from the settler is recycled back to the reactor with a purge stream or water removal unit provided to account for the water added to the extractor and in the fresh aqueous feed. Note that the aqueous stream from the settler has very little catalyst. Therefore, catalyst loss through the purge stream is minimal. The requirements for the successful operation of this flowsheet are as follows:

- The ion pairs QX and QY should be organophilic enough to reside almost completely in the organic phase of the LLPTC reactor.
- The ion pairs should also be sufficiently hydrophilic to go almost completely into the aqueous phase in the extractor.

In the Class II flowsheet (Figure 13), as before, the aqueous and organic phases are separated in the settler that follows the LLPTC reactor. The organic stream from the settler contains almost all of the phase transfer catalyst. The product is removed from this stream (by distillation) and the remainder (catalyst, solvent, and unconverted reactant) is sent back to the reactor. The aqueous stream from the settler is recycled back to the reactor. A modification of this flowsheet is shown in Figure 14. Here, after product removal, the organic stream is used to extract whatever little amount of catalyst that remains in the aqueous phase. The fresh aqueous feed is added just prior to the extractor and the purge stream is removed from the aqueous stream from the extractor. The requirements for the successful operation of Class II flowsheets are as follows:

- The ion pairs QX and QY should be highly organophilic so as to reside almost completely in the organic phase of the LLPTC reactor.
- The reaction product should be easy to separate by distillation (preferably the lightest boiler).
- The reaction product should be volatile enough or the catalyst should be stable enough to be able to withstand the

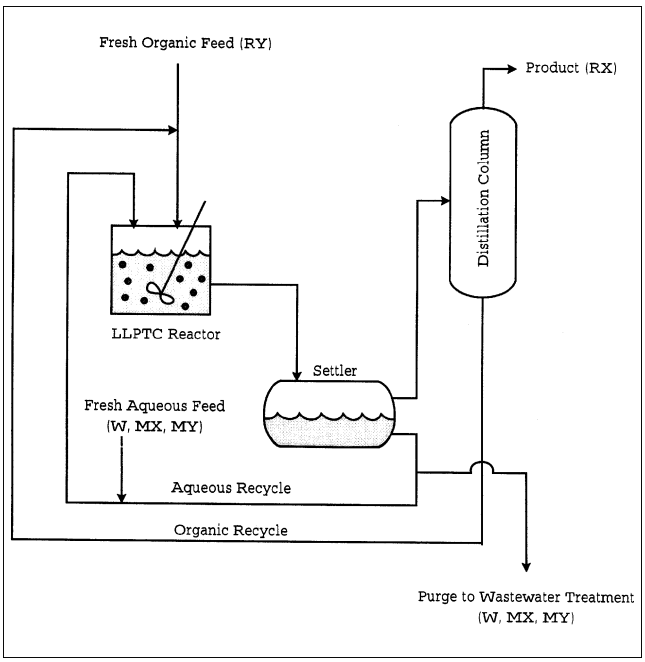

Figure 13. Class II flowsheet for a LLPTC process with catalyst recovery and recycle.

distillation temperature (PT catalysts, especially quaternary ammonium salts, have a tendency to decompose at higher temperatures).

Figure 15a shows the fractional amount of Q^+ fed to the system that appears in the aqueous product stream of the stirred cell as a function of the mole fraction of cation M^+ in

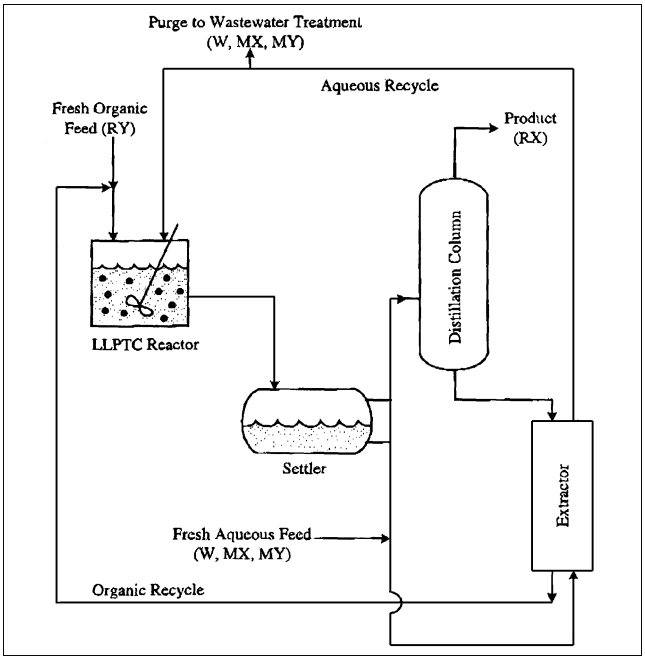

Figure 14. Modified Class II flowsheet for a LLPTC process with catalyst recovery and recycle.

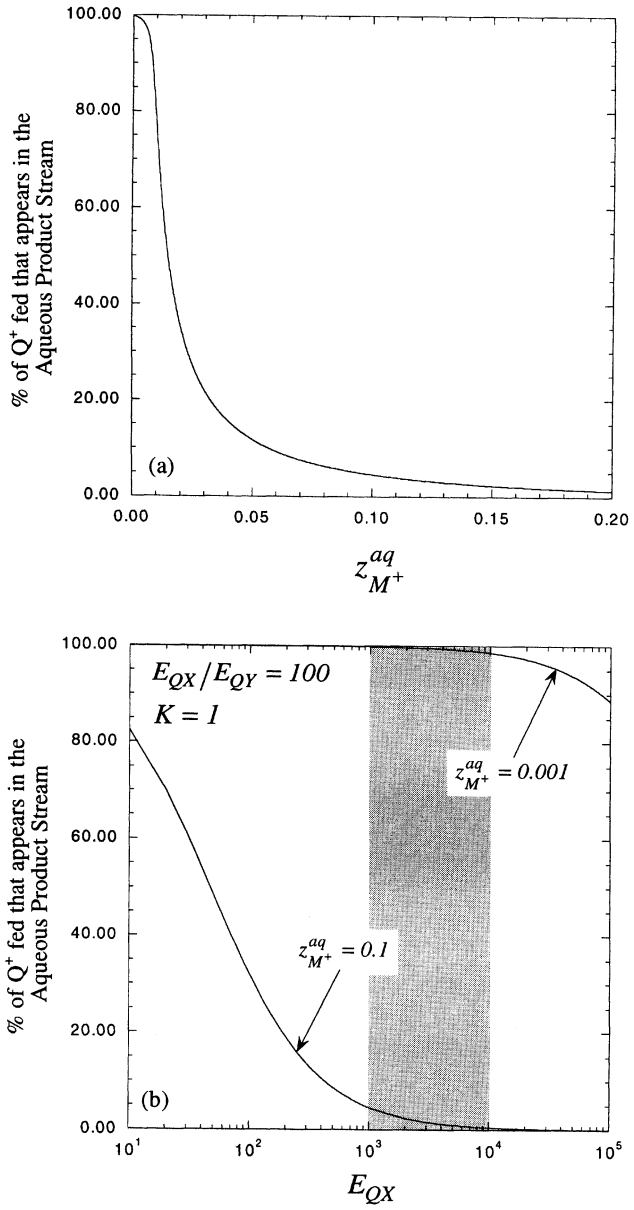

Figure 15. Catalyst recovery aspects.

(a) Distribution of Q^+ into the aqueous and organic phases as a function of $z^{aq}_{M^+}$; (b) feasibility of operation of the Class I flowsheet.

the aqueous feed. The remaining amount of Q^+ appears in the organic phase. Base-case values (Table 1) of the thermodynamic parameters are used. For high values of $z^{aq}_{M^+}$, most of the catalytic cation partitions into the organic phase. As the concentration of M^+ in the aqueous feed decreases, more and more Q^+ starts to appear in the aqueous phase. In the limit of pure water as the aqueous feed, Q^+ partitions almost completely into the aqueous phase. This result shows that we can manipulate the distribution of the catalytic cation into the aqueous and organic phases by manipulating the concentration of the aqueous-phase cation M^+. This fact is utilized in the operation of the extractor in the modified Class II flowsheet (Figure 14). The fresh aqueous feed (which con-

Table 2. Guidelines for Using Catalyst Recovery and Recycle Flowsheets

Class I
• Use when the catalyst is thermally unstable and has to be completely separated before product removal. • Choose catalyst with $10^3 \le E_{QX} \le 10^4$.
Class II
• Use when the catalyst is thermally stable. • Use when product is volatile and easily separable by distillation (preferably lightest boiler). • Use catalyst with $E_{QX} \ge 10^3$. • Use Class II (Figure 13) for $E_{QX} \ge 10^4$. • Use modified Class II (Figure 14) for $10^3 \le E_{QX} \le 10^4$.

tains M^+) is introduced just prior to the extractor. The increased concentration of M^+ in the aqueous phase forces whatever little amount of Q^+ that is left in the aqueous phase into the organic phase, thereby improving the catalyst recovery.

Figure 15b shows the distribution of Q^+ into the aqueous and organic phases as a function of E_{QX} (for a fixed E_{QX}/E_{QY}) for a high ($=0.1$) and a very low ($=0.001$) value of $z^{\text{aq}}_{M^+}$. For Class I flowsheet, the high value of $z^{\text{aq}}_{M^+}$ corresponds to the LLPTC reactor operation and the low value of $z^{\text{aq}}_{M^+}$ corresponds to the operation of the extractor in which the organic phase is contacted with a fresh water stream. In the LLPTC reactor, we want the catalytic cation Q^+ to partition almost completely into the organic phase. Clearly, high values of E_{QX} ($>10^3$) are needed for this purpose. In the extractor, we want the catalytic cation to partition almost completely into the aqueous phase. However, as E_{QX} increases beyond 10^4, Q^+ becomes so organophilic that this is no longer possible. Therefore, for successful operation of the Class I flowsheet E_{QX} should be such that $10^3 \le E_{QX} \le 10^4$ (shaded region in Figure 15b). The guidelines for using the two classes of flowsheets that we have developed are summarized in Table 2.

These results help us understand the LLPTC process better. Next, let us see how this understanding can be used for selection of the phase attributes, the catalyst, and the organic solvent.

Choice of Reactor Attributes

Typically, industrial LLPTC processes are carried out in a CSTR accompanied by a settler. Many processes are operated in the batch mode. However, incentive for continuous operation exists, and it has been used (Stanley and Quinn, 1987; Reed and Snedecor, 1995; Naik and Doraiswamy, 1998). In some cases, use of multiple stages and other reactor types (Matson and Stanley, 1988; Samant and Ng, 1998a) may also be advantageous. Here, as the reactor type is fixed, we are left with the task of selecting the most suitable phase attributes. In addition, we would like to choose the PT catalyst and the organic solvent.

Choice of phase attributes

The phase attributes of interest are:

- Choice of the dispersed and continuous phases
- Mean drop size of the dispersed phase
- Dispersed and continuous-phase holdups
- Residence time or reactor size.

Table 3. Pros and Cons of Organic-in-Aqueous and Aqueous-in-Organic Systems

Dispersed Phase	Pros	Cons
Organic	• Higher conversion*	• Smaller reactive holdup* • Higher settling time** • Higher power requirement**
Aqueous	• Larger reactive holdup* • Lower settling time • Lower power requirement	• Lower conversion*

*Dispersed phase typically has the smaller molar holdup. Therefore, the conversion is high when $H^{\text{aq}}/H^{\text{org}}$ is high; that is, when when the organic phase is dispersed (Figure 11). However, when the organic phase is dispersed, the reactive holdup is smaller. Therefore, for a given reactor size, the total production could be lower.
**Walas (1988).

The most significant phase attribute is the choice of the dispersed and continuous phases. In most LLPTC applications studied experimentally, the organic phase is traditionally dispersed into the aqueous phase. However, dispersing the aqueous phase into the organic phase may be advantageous in some cases. The pros and cons of organic-in-aqueous and aqueous-in-organic systems are listed in Table 3.

The organic (reactive) phase Damköhler numbers for reaction and mass transfer (Eq. 24) can be rewritten in the following form

$$Da^{\text{org}}_r = \tau^{\text{org}} k_f$$
$$Da^{\text{org}}_{m_i} = \tau^{\text{org}} a^{\text{org}}_s K^{I\text{org}}_{m_i}, \qquad \forall i \tag{35}$$

By assuming the mass-transfer coefficients for all components to be the same, we can write

$$\frac{Da^{\text{org}}_r}{Da^{\text{org}}_m} = \frac{1}{a^{\text{org}}_s}\frac{k_f}{K^{I\text{org}}_m}$$
$$Da^{\text{org}}_m = \tau^{\text{org}} a^{\text{org}}_s K^{I\text{org}}_m \tag{36}$$

Equation 36 relates the Damköhler numbers to the phase attributes (through a^{org}_s and τ^{org}) and the rate parameters of the reaction system under consideration (k_f, $K^{I\text{org}}_m$). LLPTC processes give the best results in the thermodynamic limit. Therefore, once the dispersed phase is chosen, we must choose the remaining phase attributes so as to obtain high values for $Da^{\text{org}}_r/Da^{\text{org}}_m$ and Da^{org}_m. Guidelines for this task were presented by Samant and Ng (1998b) and will not be repeated here. The choices made depend on the values of k_f and $K^{I\text{org}}_m$, which in turn depend on the PT catalyst and the organic solvent. Therefore, the choice of phase attributes and the choice of catalyst and solvent are interlinked.

Choice of PT catalyst and organic solvent

The catalyst and solvent choices are laboratory-scale decisions. They must be chosen and fixed when we decide to take

Table 4. Commonly Used LLPTC Catalysts*

Catalyst	Salient Features
Quaternary Ammonium Salts (Quats)	• Cheap • Moderately stable (up to ~100°C) • Moderately reactive • Widely used
Phosphonium Salts	• Costlier than quats • More stable thermally than quats • Widely used
Crown ethers	• Expensive • Stable (even up to ~150–200°C) • Highly reactive • Environmental issues due to toxicity • Often used
Cryptands	• Expensive • Stable • Highly reactive • Environmental issues due to toxicity • Used sometimes
PEG	• Very cheap • More stable thermally than quats • Easier to recover than quats • Often used

*Adapted from Naik and Doraiswamy (1998).

the process to the pilot-plant or commercial scale. The choice of the catalyst affects the rate parameters such as k_f and $K_m^{I\text{org}}$ and thermodynamic parameters such as E_{QX}, E_{QY}, and K. The choice of the organic solvent affects k_f, E_{QX}, E_{QY}, and the ratio E_{QX}/E_{QY}.

Note that in choosing a catalyst, we are choosing only the catalytic cation Q^+. The anions X^- and Y^- are fixed by the organic reactant (RY) and the desired product (RX). Therefore, the choice of the catalyst does not affect E_{QX}/E_{QY}, although it affects the individual values of E_{QX} and E_{QY} (see Eq. 19). (It is interesting to note that in general, the reactant chosen (RY) is such that the anion Y^- is smaller and harder (larger charge-to-volume ratio) than the anion X^-. Smaller and harder anions are more strongly hydrated and therefore less organophilic. Therefore, such choice results in higher values of E_{QX}/E_{QY}.) Also, for most LLPTC processes, K is fairly high. Therefore, we will not consider it as a factor in choosing the catalyst.

The aspects that need to be considered in evaluating PT catalysts and organic solvents are:

- Reactivity and stability
- Cost and availability
- Recovery and recycle
- Toxicity and environmental considerations.

Some commonly used catalysts and their salient features are noted in Table 4. In terms of reactivity, stability, widespread availability, and costs, quaternary ammonium salts (quats) are the most effective and feasible PT catalysts, and are often the catalyst of choice in industrial operations. Let us now see how the structural properties of a quat and the properties of an organic solvent are correlated to the rate and thermodynamic parameters.

Catalyst Structural Properties. Quaternary ammonium cations have four alkyl chains attached to a nitrogen atom (+ ve center). The two important parameters that characterize the quat structure are (Starks et al., 1994; Halpern, 1997)

$$p = \sum_{i=1}^{4} C_i \qquad \text{(Bulkiness Parameter)}$$

$$q = \sum_{i=1}^{4} \frac{1}{C_i} \qquad \text{(Accessibility Parameter)} \tag{37}$$

C_i is the number of carbon atoms on chain i.

The bulkiness parameter p is the total number of carbon atoms on the quat cation. In general, as the bulkiness (p) increases, the organic nature and the organophilicity of the quat cation increase. Therefore, E_{QX} and E_{QY} increase with increasing p. As the cation becomes bulkier, its association with the anions in the ion pairs becomes weaker. This increases the reactivity (k_f). Also, the resistance to mass transfer is higher for bulkier cations. Therefore, $K_m^{I\text{org}}$ decreases with increasing p.

q is known as the accessibility parameter. The nitrogen atom (+ ve center) is considered increasingly accessible to the −ve center of the anions as the alkyl chains of the quat become shorter with particular significance to the shortest alkyl chain. For example, let us consider a tetrabutylammonium ion ($p=16,\ q=1$). Here, the nitrogen atom is surrounded by four bulky butyl chains, thus making it relatively inaccessible to the anions. On the other hand, consider a tripentylmethylammonium ion ($p=16,\ q=1.6$). It has the same number of carbon atoms as the tetrabutylammonium ion. However, it has only three bulky chains and there is one short chain (methyl), which leaves the nitrogen atom relatively more accessible to the anions. In general, for a given p, the accessibility increases as q increases. The increased accessibility affects the rate and thermodynamic parameters as follows. As the quat cation becomes more accessible, it is more strongly associated with the anions in the ion-pairs. This leads to reduction in k_f. The accessible face of the cation can easily sit on the organic-aqueous interface, thereby reducing the interfacial tension (Mason et al., 1990; Starks et al., 1994). Therefore, $K_m^{I\text{org}}$ increases with increasing accessibility (in our opinion, more evidence is clearly needed to support this observation). The increased accessibility of the + charge on the quat cation also increases its tendency to be hydrated. Therefore, the organophilicity (E_{QX} and E_{QY}) decreases with increasing accessibility.

Table 5 summarizes the effects of the quat cation structure on the rate and thermodynamic parameters.

Solvent Properties. The important properties of the organic solvent are its polarity and its dielectric constant (Morrison and Boyd, 1983). The effects of these properties on the rate and thermodynamic parameters are also summarized in Table 5.

In the organic phase, each ion of the ion-pair is surrounded by a cluster of solvent molecules and is said to be solvated. In solvents of high polarity and high dielectric constant (high insulating properties to lower the attraction between oppositely charged solvated ions), the solvation is stronger and a layer or layers of insulating solvent molecules may separate the pair of ions. The association between the ions of the ion pair is therefore weaker, and, hence, k_f is

Table 5. Effect of Catalyst and Solvent Properties

Property	Effect* on k_f	$K_m^{I\text{org}}$	E_{QX}	E_{QY}	$\frac{E_{QX}}{E_{QY}}$
Catalyst Structural Properties					
p (Bulkiness)	↑	↓	↑	↑	—
q (For given p) (Accessibility)	↓	↑	↓	↓	—
Solvent Properties					
Polarity	↑	—	↑	↑	↓
Dielectric constant	↑	—	↑	↑	↓

*All effects are with increase in the property value.

higher. On the other hand, in solvents of low polarity, where the solvation is weak, there are no solvent molecules between the pair of ions and the ionic bonding is strong. Therefore, k_f is lower.

The increase in strength of solvation also increases the organophilicity of the ion-pairs. Therefore, E_{QX} and E_{QY} increase with an increase in the polarity and the dielectric constant of the solvent. However, the increase in the strength of solvation is more pronounced for the smaller and harder anion Y^- than for the larger and softer anion X^-. Therefore, although the individual values of E_{QX} and E_{QY} increase, the ratio E_{QX}/E_{QY} typically decreases.

Recommendations for Catalyst and Solvent Selection. There are no universally applicable criteria for choosing the optimal catalyst and organic solvent for LLPTC processes. In general, a number of PT catalysts and organic solvents need to be screened for the reaction system under consideration. However, based on the discussion so far (see Tables 2, 3 and 5), we can make some recommendations for this purpose. These recommendations are summarized in Tables 6 and 7.

First let us briefly go through the recommendations for choosing the organic solvent. As indicated in Table 6, a solvent is not needed when the organic phase reactants and products are in liquid phase at the temperature and pressure of operation. We have noted that high values of E_{QX}/E_{QY} are required to obtain high conversion in the thermodynamic limit. A polar solvent with a high dielectric constant enhances the rate parameters (k_f) and the equilibrium distribution coefficients (E_{QX}, E_{QY}), but decreases the ratio E_{QX}/E_{QY}. In other words, it facilitates the approach to the thermodynamic equilibrium, but worsens the performance in the thermodynamic limit. The approach to the thermodynamic limit can be facilitated by adjusting the phase attributes (a_s^{org}, τ^{org}, Eq. 36) as shown by Samant and Ng (1998b). Therefore, the main criterion of interest in selecting a solvent is not the approach to thermodynamic equilibrium, but the performance in the thermodynamic limit. Therefore, nonpolar solvents such as cyclohexane, toluene are preferred. However, when the anion X^- (and, therefore, Y^-) is small and hard (very hydrophilic), the values of k_f, E_{QX}, and E_{QY} are very low for nonpolar solvents. In such as cases, a polar solvent with high dielectric constant is recommended in order to get reasonably high values of k_f, E_{QX}, and E_{QY}.

Table 6. Recommendations for Selecting the Organic Solvent

- Do not use solvent if the organic reactants and products (RX and RY) exist in liquid phase at the temperature and pressure of operation
- Use an environmentally benign solvent
- Do not use a solvent that is miscible with water
- Use a solvent that is easily separable (preferably heavy boiler)
- Use a nonpolar solvent (such as cyclohexane, toluene) when the anion Y^- is large and soft (such as Br^-, I^-)
- Use a polar solvent with high dielectric constant (such as MIBK) when the anion X^- is small and hard (such as F^-)

Table 7. Recommendations for Selecting the PT Catalyst (Quat)

Choice of Recovery Scheme	Choice of Dispersed Phase	Choice of Structural Parameters
Class I	Organic	$16 \le p \le 24$, $q \le 1$ preferably, symmetric quats such as tetrabutyl ammonium
	Aqueous	$p \ge 16$, $q > 1$. asymmetric quats such as trioctylmethyl ammonium
Class II	Organic	$p \ge 24$, $q \le 1$. preferably, symmetric quats such as tetrahexyl ammonium
	Aqueous	$p \ge 24$, $q > 1$. asymmetric quats such as trioctylmethyl ammonium
Modified Class II	Organic	$16 \le p \le 24$, $q \le 1$. preferably, symmetric quats such as tetrahexyl ammonium
	Aqueous	$p \ge 16$, $q \ge 1$. asymmetric quats such as trioctylmethyl ammonium.

Let us now turn our attention to the recommendations for selecting quaternary ammonium catalysts (Table 7). These recommendations depend upon the choice of recovery scheme (Table 2) and dispersed phase (Table 3). Let us consider a case where the product is non-volatile and the catalyst has to be completely separated from the organic phase before the product is removed. Therefore, we have to use the Class I flowsheet for catalyst recovery and recycle. Let us first choose the organic phase to be the dispersed phase. When the organic phase is dispersed, a_s^{org} is high. Therefore, the rate parameter of importance is k_f (Eq. 36). In order to make $Da_r^{\text{org}}/Da_m^{\text{org}}$ as high as possible, we have to choose a high value of k_f. $K_m^{I\text{org}}$ is not so important here as a_s^{org} is high. For getting high values of k_f, we prefer bulky, less accessible quats. Therefore, symmetric quats with $q \le 1$ are recommended. Also, for feasible operation of the Class I flowsheet, we need $10^3 \le E_{QX} \le 10^4$. Therefore, quats with $16 \le p \le 24$ are recommended. Let us now see how the choice of aqueous phase as the dispersed phase affects our decisions. Here, a_s^{org} is low. Therefore, increasing $K_m^{I\text{org}}$ is much more important than increasing k_f (Eq. 36). Therefore asymmetric, highly ac-

cessible quats with $q > 1$ are recommended. $p \geq 16$ is recommended in order to have $E_{QX} \geq 10^3$. Note that E_{QX} is generally low for asymmetric quats, even for high values of p. Therefore, we do not put an upper bound on the recommended value of p. Other recommendations are based on similar logical reasoning. We will not go through them in detail for the sake of brevity.

Conclusions

Phase transfer catalysis plays a significant role in the synthesis of fine chemicals. Yet, relatively little is available on its engineering analysis, particularly on the exploitation of the chemistry of PTC and the recovery of PT catalysts (Naik and Doraiswamy, 1998). This study attempts to address some of these issues from a conceptual design point of view.

A stirred cell model is formulated to understand the effect of reaction kinetics, mass transfer, and thermodynamics on the performance of a LLPTC reaction system. This analysis identifies the Damköhler number for mass transfer, the Damköhler number for reaction, the catalyst equilibrium distribution coefficients, and the reaction equilibrium constant to be the parameters for characterizing the system. The values of these parameters leading to good reactor performance are identified. These parameters are in turn related to the reactor attributes such as the choice of the dispersed phase, drop size, and phase holdups. Then, for the conceptual design of a reactor, one can work in reverse by selecting reactor attributes that would lead to the parameter values that correspond to desired reactor performance.

Similarly, these characterizing parameters are related to the molecular properties of the catalyst (bulkiness and accessibility), as well as those of the solvent (polarity and dielectric constant). Recommendations for selecting catalyst and solvent for enhanced reactor performance are provided. Two classes of catalyst recycle schemes have been identified and can be selected based on the values of the catalyst distribution coefficients and the thermal stability of the catalyst.

This study represents our continuing effort to study reaction system synthesis from a multiscale perspective (Lerou and Ng, 1996). For optimal reaction system synthesis, issues at four different length scales need to be considered—plant, reactor, catalyst, and molecular. We turn reactor analysis into synthesis of reactor attributes and operating conditions in a systematic manner. At the plant scale, the recovery and recycle of catalyst and unconverted reactant are considered. At the catalyst and molecular scales, we exploit the molecular properties of the PT catalyst, as well as the solvent for enhanced performance. Further effort is under way to integrate reactor design and process systems engineering.

Acknowledgments

We express our appreciation to the National Science Foundation, grant No. CTS-9807101, for support of this research.

Notation

a = total interfacial surface area for mass transfer, m^2
a_s = specific interfacial surface area for mass transfer, 1/m
c_T = total liquid phase concentration, mol/m^3
C = number of carbon atoms
$Da_{m_i}^{\phi}$ = Damköhler number for mass transfer of component i in phase ϕ
Da_r^{ϕ} = Damköhler number for reaction in phase ϕ
E = equilibrium distribution coefficient
F = molar flow rate of feed stream, mol/s
P = molar flow rate of product stream, mol/s
H^{ϕ} = molar holdup of phase ϕ, mol
$\bar{J}_i$ = molar flux of component i relative to the molar average velocity, mol/m^2s
$\bar{J}_T$ = total molar flux relative to the molar average velocity, mol/m^2s
k_f = forward reaction rate constant 1/s
k_r = reverse reaction rate constant 1/s
K = thermodynamic reaction equilibrium constant
$K_{m_i}^I$ = coefficient for mass transfer of component i across the interface, m/s
$K_{m_{ij}}^I$ = coefficient for mass transfer of component i across the interface due to the gradient in composition of component j, m/s
M = molecular weight
n_i = number of moles of apparent component i, mol
n_{TOT} = total number of apparent moles, mol
$\hat{n}_i$ = number of moles of real component i, mol
$\hat{n}_{TOT}$ = total number of real moles, mol
$\bar{N}_i$ = molar flux of component i relative to stationary coordinates, mol/m^2s
$\bar{N}_T$ = total molar flux relative to stationary coordinates, mol/m^2s
p = bulkiness parameter
q = accessibility parameter
$r(\boldsymbol{x})$ = rate of reaction per mole of reaction mixture of composition $\boldsymbol{x}$, 1/s
R = universal gas constant
T = temperature, K
x_i, z_i = mole fraction of component i
Δx_i^{ϕ} = composition difference driving force in phase ϕ
X = conversion
γ_i = activity coefficient of component i
μ_i = chemical potential of component i
τ = average residence time, s
υ_i = stoichiometric coefficient of component i

Subscripts

aq = aqueous phase
i, j = component indices
org = organic phase
ϕ = phase index

Superscripts

aq = aqueous phase
F = feed
I = interface
P = product
org = organic phase
ϕ = phase index

Literature Cited

Berris, B. C., "Phase Transfer Catalyst Recovery," U.S. Patent No. 5,030,757 (July 9, 1991).
Brändström, A., "Principles of Phase Transfer Catalysis by Quaternary Ammonium Salts," *Adv. Phys. Org. Chem.*, **15**, 267 (1977).
Dehmlow, E. V., and S. S. Dehmlow, *Phase Transfer Catalysis*, VCH, Germany (1993).
Freedman, H. H., "Industrial Applications of Phase Transfer Catalysis (PTC): Past, Present, and Future," *Pure Appl. Chem.*, **58**, 857 (1986).
Halpern, M. E., "Integrated Guideline for Choosing a Quaternary Ammonium Salt as a Phase Transfer Catalyst to Enhance Reactivity and Separation," *Phase Transfer Catalysis: Mechanisms and Syntheses*, M. E. Halpern, ed., ACS Symp. Ser., No. 659 (1997).
Johnson, K. L., "Cyclic Process for Activation, Use, and Recovery of Phase Transfer Catalysts," U.S. Patent No. 5,483,007 (Jan. 9, 1996).

Johnson, K. L., "Cyclic Process for Activation, Use, and Recovery of Phase Transfer Catalysts," U.S. Patent No. 5,675,029 (Oct. 7, 1997).
Krishna, R., and R. Taylor, "Multicomponent Mass Transfer: Theory and Applications," *Handbook of Heat and Mass Transfer*, Vol. 2, N. P. Cheremisinoff, ed., Gulf Publishing, Houston (1986).
Lerou, J. J., and K. M. Ng, "Chemical Reaction Engineering: A Multiscale Approach to a Multiobjective Task," *Chem. Eng. Sci.*, **51**, 1595 (1996).
Makosza, M., "Two-Phase Reactions in the Chemistry of Carbanions and Halocarbenes: A Useful Tool in Organic Synthesis," *Pure Appl. Chem.*, **43**, 439 (1975).
Mason, D., S. Magdassi, and Y. Sasson, "Interfacial Activity of Quaternary Salts as a Guide to Catalytic Performance in Phase Transfer Catalysis," *J. Org. Chem.*, **55**, 2714 (1990).
Masuko, F., H. Yamachika, K. Fujiyoshi, and K. Shiota, "Recovery of Catalyst," U.S. Patent No. 4,172,782 (Oct. 30, 1979).
Matson, S. L., and T. J. Stanley, "Phase Transfer Catalysis," U.S. Patent No. 4,754,089 (Jun. 28, 1988).
Morrison, R. T., and R. N. Boyd, *Organic Chemistry*, 4th ed., Allyn and Bacon, MA (1983).
Naik, S. D., and L. K. Doraiswamy, "Phase Transfer Catalysis: Chemistry and Engineering," *AIChE J.*, **44**, 612 (1998).
Pitzer, K. S., *Thermodynamics*, 3rd ed., McGraw Hill, New York (1995).
Reed, D. J., and T. G. Snedecor, "Process to Produce Vinylidene Chloride Using Phase Transfer Catalyst," U.S. Patent No. 5,396,002 (Mar. 7, 1995).
Reuben, B., and K. Sjöberg, "Phase Transfer Catalysis in Industry," *Chemtech*, **41**, 315 (1981).
Samant, K. D., and K. M. Ng, "Synthesis of Extractive Reaction Processes," *AIChE J.*, **44**, 1363 (1998a).
Samant, K. D., and K. M. Ng, "Effect of Kinetics and Mass Transfer on Design of Extractive Reaction Processes," *AIChE J.*, **44**, 2212 (1998b).
Stanley, T. J., and J. A. Quinn, "Phase Transfer Catalysis in a Membrane Reactor," *Chem. Eng. Sci.*, **42**, 2313 (1987).
Starks, C. M., "Phase Transfer Catalysis: I. Heterogeneous Reactions Involving Anion Transfer by Quaternary Ammonium and Phosphonium Salts," *J. Amer. Chem. Soc.*, **93**, 195 (1971).
Starks, C. M., C. L. Liotta, and M. Halpern, *Phase-Transfer Catalysis: Fundamentals, Applications, and Industrial Perspectives*, Chapman and Hall, New York (1994).
Walas, S. M., *Chemical Process Equipment. Selection and Design*, Butterworth Publishers, MA (1988).

Manuscript received July 7, 2000, and revision received Feb. 5, 2001.